LASER INTERFEROMETER GRAVITATIONAL WAVE OBSERVATORY
- LIGO -
CALIFORNIA INSTITUTE OF TECHNOLOGY
MASSACHUSETTS INSTITUTE OF TECHNOLOGY

2023/08/23

INTERIM REPORT 2

Sophia Adams

California Institute of Technology
LIGO Project, MS 18-34
Pasadena, CA 91125
Phone (626) 395-2129
Fax (626) 304-9834
E-mail: info@ligo.caltech.edu

Massachusetts Institute of Technology
LIGO Project, Room NW22-295
Cambridge, MA 02139
Phone (617) 253-4824
Fax (617) 253-7014
E-mail: info@ligo.mit.edu

LIGO Hanford Observatory
Route 10, Mile Marker 2
Richland, WA 99352
Phone (509) 372-8106
Fax (509) 372-8137
E-mail: info@ligo.caltech.edu

LIGO Livingston Observatory
19100 LIGO Lane
Livingston, LA 70754
Phone (225) 686-3100
Fax (225) 686-7189
E-mail: info@ligo.caltech.edu

http://www.ligo.caltech.edu/

Quality Testing Optically Contacted Bonds

Sophia Adams, Caltech

Mentor: Professor Rana Adhikari, Caltech
Contributors: MacMillan, Ian, Caltech; Markowitz, Aaron, Caltech

Abstract

Optical contacting is a type of bonding that can be achieved when flat, polished surfaces are brought into close contact. When used as a replacement for fused silica, optically contacted silicon has the potential to increase the sensitivity of LIGO Voyager to gravitational waves. This project is aimed at determining the quality factor of optically contacted silicon bonds in order to quantify their potential to reduce the noise in LIGO Voyager. By maximizing the energy contribution from the bond and oscillating a silicon cantilever, the quality factor of the bond can be estimated. The eventual goal is to create an ideal optically contacted bond which minimizes damping and energy loss.

1 Experimental Setup

This project focuses on testing the mechanical loss of an optically contacted bond within a silicon wafer. The silicon wafer cantilever will be given an initial impulse, and the ring-down will be measured. The quality factor (the inverse of the mechanical loss) can be obtained from a measure of how damped the response is. In order to measure the oscillations of the cantilever, an optical lever was setup as in figure 1.

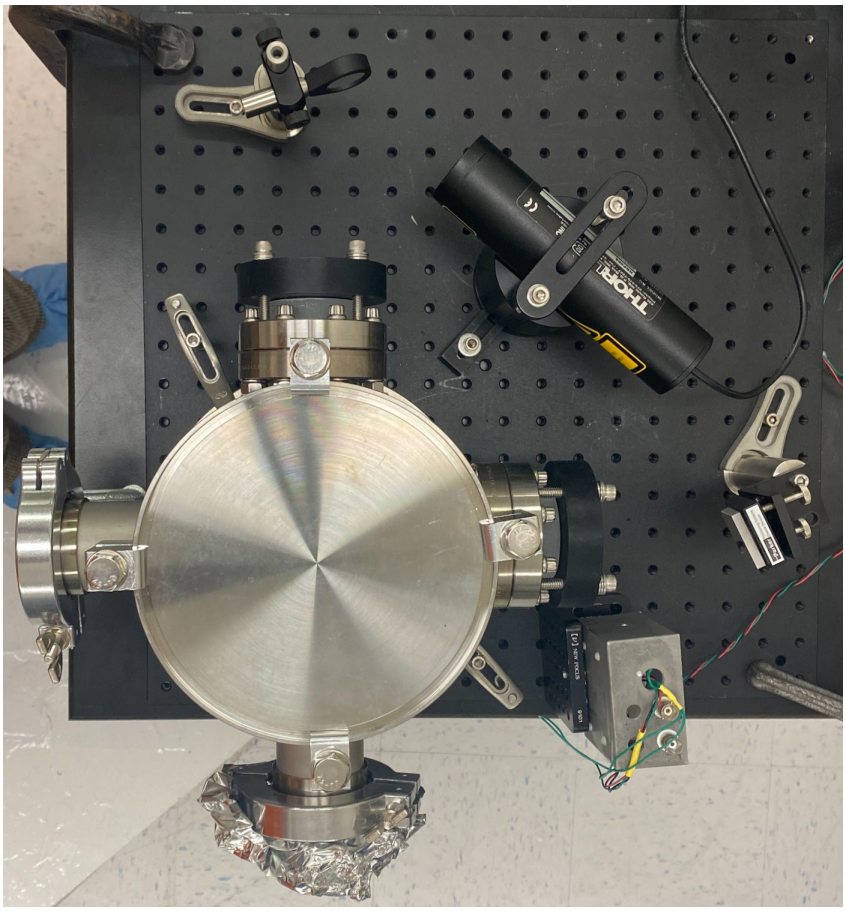

Figure 1: Experimental setup for measurement of ring-down. Notice the laser beam hits a mirror and is then directed into a vacuum chamber containing a silicon rectangular cantilever which is clamped. The beam then hits another mirror and is directed into a photo diode connected to a power supply and a Moku which acts as an oscilloscope.

2 Cantilever Geometry

In order to make the measurement of the quality factor of the bond precise, the energy in the bond should be maximized while the energy in the rest of the system (the silicon and the clamp) should be minimized. An appropriate geometry should be selected for this purpose.

Gentle nodal suspension is an experimentally tested way of measuring the quality factor of a substrate [1]. However, gentle nodal suspension fails at cryogenic temperatures, which have been shown to yield high Q measurements.

Three different cantilever geometries were analyzed in order to find a suitable energy ratio between the bond and the rest of the silicon wafer. The ratio between shear and bending energy was estimated for the geometries shown in figure 2 using the following equations where M is the moment, I is the moment of inertia, l is the length, E is young's modulus, K is a constant that depends on the geometry (1.11 for circular and 0.5 for rectangular sections), V is the traverse shear force, G is the modulus of rigidity, and A is the cross sectional area.

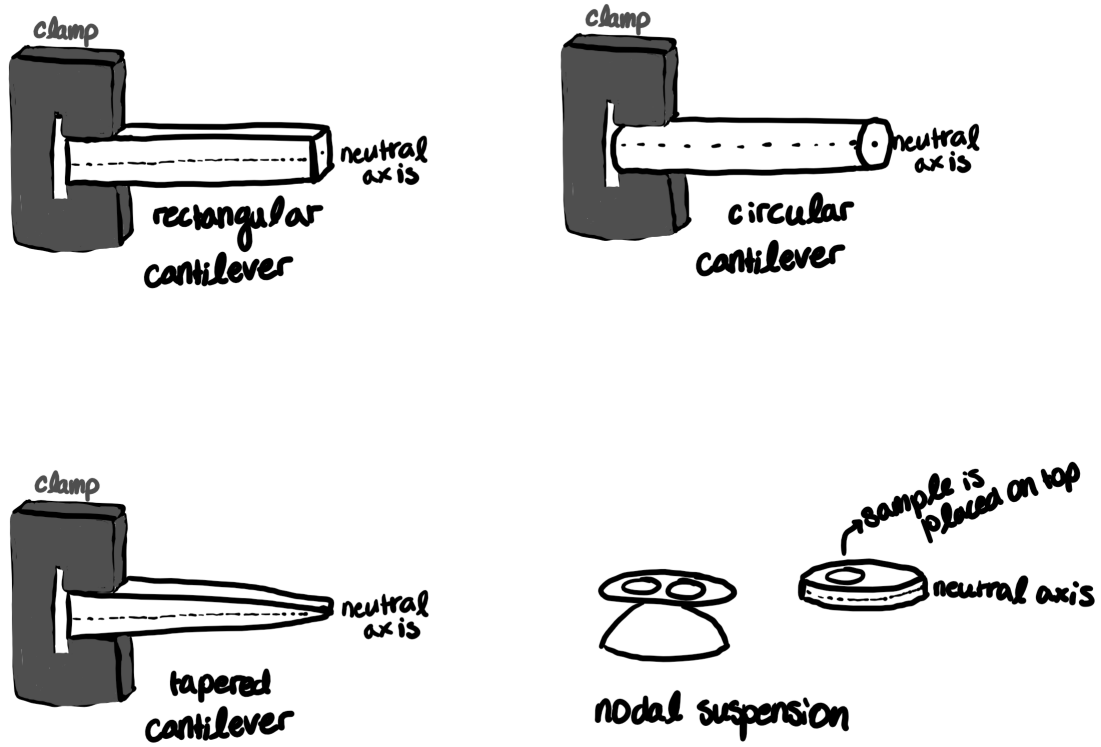

Figure 2: A diagram of three sample cantilever geometries and the setup for gentle nodal suspension.

$constant\ bending\ energy = \frac{M^2 l}{2EI}$

$constant\ traverse\ shear\ energy = \frac{KV^2 l}{2GA}$

A tapered cantilever was selected to maximize shear stress and minimize bending. In a tapered cantilever, the bond in the middle will experience maximum shear stress, and the whole cantilever will have its bending stress minimized. However in general, the bending stress in a cantilever is greater than the shear stress. The actual ratio was determined using finite element analysis in COMSOL. The results are presented in the following sections.

2.1 Pizza Cantilever

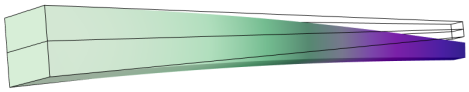

Figure 3: Stresses on a pizza cantilever at 34557 Hz.

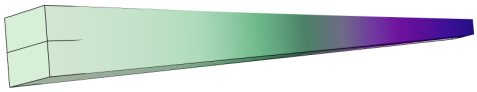

Figure 4: Stresses on a pizza cantilever at 51994 Hz.

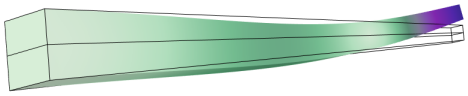

Figure 5: Stresses on a pizza cantilever at 1.0385E5 Hz.

Figure 6: Stresses on a pizza cantilever at 1.5129E5 Hz.

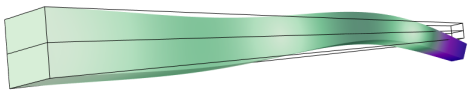

Figure 7: Stresses on a pizza cantilever at 2.1981E5 Hz.

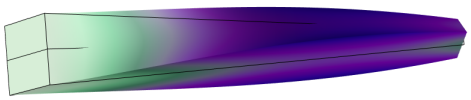

Figure 8: Stresses on a pizza cantilever at 2.7240E5 Hz.

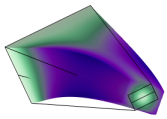

Figure 9: Stresses on a pizza cantilever at 2.7240E5 Hz viewed from the front. Note that this view is shown because the stresses are nonuniform through the center. All other eigenfrequencies have uniform stresses through their middle.

Table 1: Pizza Cantilever Energies.

Eigenfrequency (Hz)	**Bulk (N*m)**	**Shear (N*m)**	**Total (J)**	**Shear/Bulk**
34557	6.0-13	2.5E-12	1.5E-12	4.2
51994	1.4E-12	5.8E-12	3.6E-12	4.3
1.0385E5	2.8E-12	1.2E-11	7.4E-12	4.3
1.5129E5	5.8E-12	2.8E-11	1.7E-11	4.8
2.1981E5	1.0E-11	4.7E-11	2.8E-11	4.6
2.7240E5	2.1E-12	5.6E-10	2.8E-10	270

2.2 Rectangular Cantilever

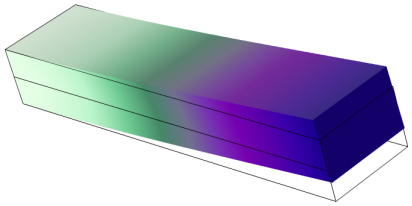

Figure 10: Stresses on a rectangular cantilever at 20385 Hz.

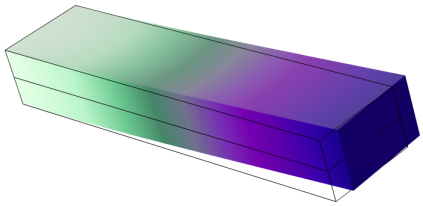

Figure 11: Stresses on a rectangular cantilever at 30507 Hz.

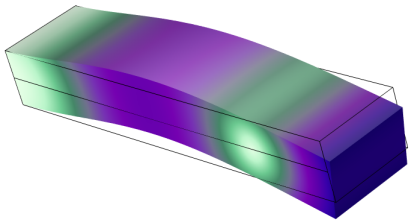

Figure 12: Stresses on a rectangular cantilever at 1.1796E5 Hz.

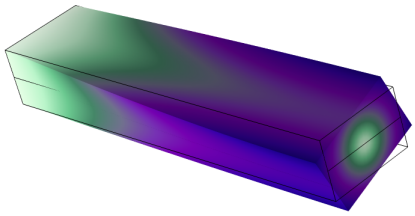

Figure 13: Stresses on a rectangular cantilever at 1.2326E5 Hz.

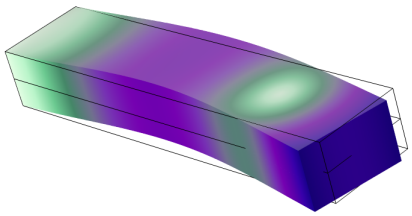

Figure 14: Stresses on a rectangular cantilever at 1.6250E5 Hz.

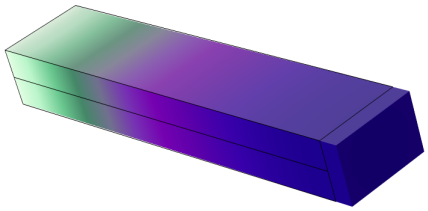

Figure 15: Stresses on a rectangular cantilever at 2.2601E5 Hz.

Table 2: Rectangular Cantilever Energies.

Eigenfrequency (Hz)	**Bulk (N*m)**	**Shear (N*m)**	**Total (J)**	**Shear/Bulk**
20385	2.2E-12	8.6E-12	5.4E-12	3.9
30507	4.8E-12	2.0E-11	1.2E-11	4.2
1.1796E5	7.3E-11	3.3E-10	2.0E-10	4.5
1.2326E5	1.4E-12	3.6E-10	1.8E-10	260
1.6250E5	1.3E-10	7.3E-10	4.3E-10	5.4
2.2601E5	5.1E-10	2.1E-9	1.3E-9	4.1

2.3 Discussion Pt. 1

For both geometries, the highest shear to bulk energy ratio was at an eigenfrequency which caused the cantilever to twist. However, looking at the graphs (figure 13 and figure 9), the highest energy contribution was from the outside edges. The next highest overall ratio was the rectangular cantilever at 1.6250E5 Hz, and the ratio was 5.420. The highest energy contribution was from the tip and the middle section.

2.4 Rectangular Cantilever With Lab Dimensions

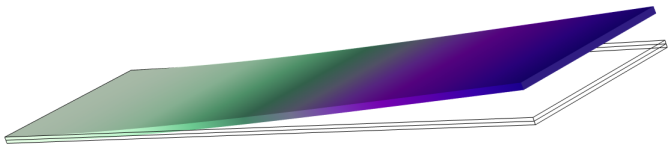

Figure 16: Stresses on a rectangular cantilever at 1266 Hz.

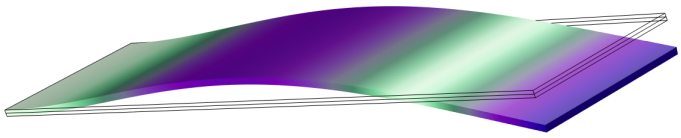

Figure 17: Stresses on a rectangular cantilever at 7927.1 Hz.

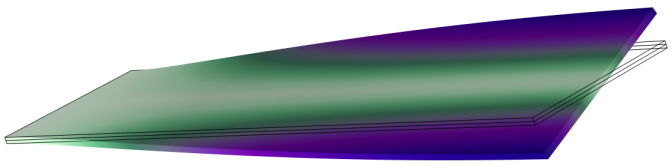

Figure 18: Stresses on a rectangular cantilever at 12012 Hz.

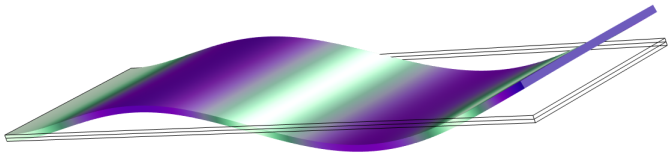

Figure 19: Stresses on a rectangular cantilever at 22212 Hz.

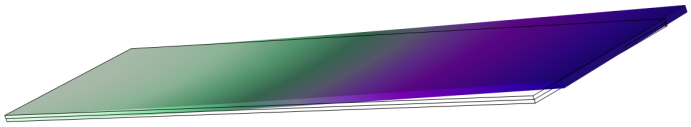

Figure 20: Stresses on a rectangular cantilever at 30433 Hz.

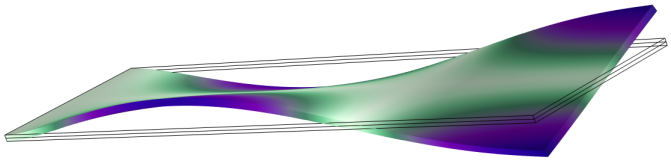

Figure 21: Stresses on a rectangular cantilever at 36767 Hz.

Table 3: Rectangular Cantilever With Lab Dimensions Energies.

Eigenfrequency (Hz)	**Bulk (N*m)**	**Shear (N*m)**	**Total (J)**	**Shear/Bulk**
1266.0	5.3E-16	1.9E-15	1.2E-15	3.6
7927.1	2.0E-14	7.6E-14	4.8E-14	3.7
12012	2.3E-15	1.4E-13	6.9E-14	58
22212	1.6E-13	5.8E-13	3.7E-13	3.6
30433	2.7E-13	1.2E-12	7.4E-13	4.5
36767	3.6E-14	1.2E-12	6.0-13	3.3

2.5 Discussion Pt. 2

The pizza cantilever with lab dimensions was not included because it is enough to make a prediction based on the data here. The trend is that the thinner the cantilever, the more vertical bending there is and the smaller the shear to bulk ratio. A pizza cantilever with the same dimensions at the base would thin out near the end and similarly have a smaller shear to bulk ratio. The data that shows this trend is included but not the images. The next step is to complete this analysis over a range of different lengths and widths in order to determine the optimal dimensions.

Table 4: Pizza Cantilever With Lab Dimensions Energies.

Eigenfrequency (Hz)	Bulk (N*m)	Shear (N*m)	Total (J)	Shear/Bulk
2085.9	1.5E-16	5.9E-16	3.7E-16	4.0
6624.0	8.0E-16	3.2E-15	2.0E-15	4.0
14820	3.4E-15	1.3E-14	8.2E-15	3.9
25628	2.6E-15	1.9E-13	9.9E-14	75
26899	1.1E-14	4.0E-14	2.5E-14	3.8
42943	2.6E-14	9.8E-14	6.2E-14	3.7

3 Parameter Estimation

An initial test of the experimental setup was conducted by gently knocking on the top of the vacuum chamber. The oscillation of the laser was measured on the oscilloscope (figure 22, figure 23), and the following analysis was performed to find the quality factor.

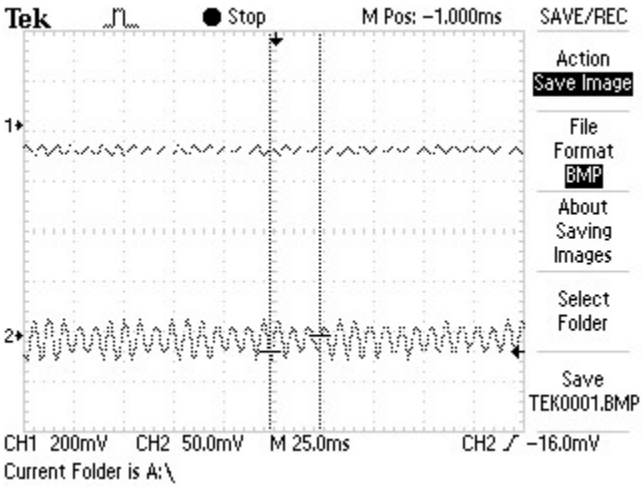

Figure 22: Oscillation of the laser after knocking the cantilever.

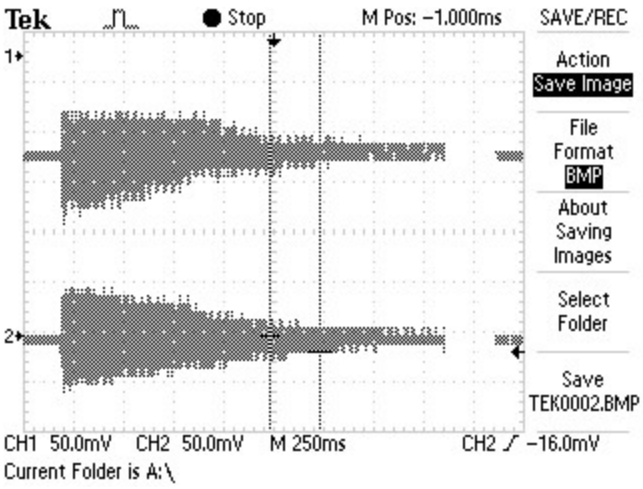

Figure 23: Oscillation of the laser zoomed out.

The signal was modeled in python using the scipy curve fit function and the following equation where ω is the angular frequency, U_0 is the initial energy, ϕ is the phase shift, and Q is the quality factor.

$$U(t) = U_0 \exp -\tfrac{\omega}{2Q} t \cos \omega t \sqrt{1 - \tfrac{1}{4Q^2}} + \phi$$

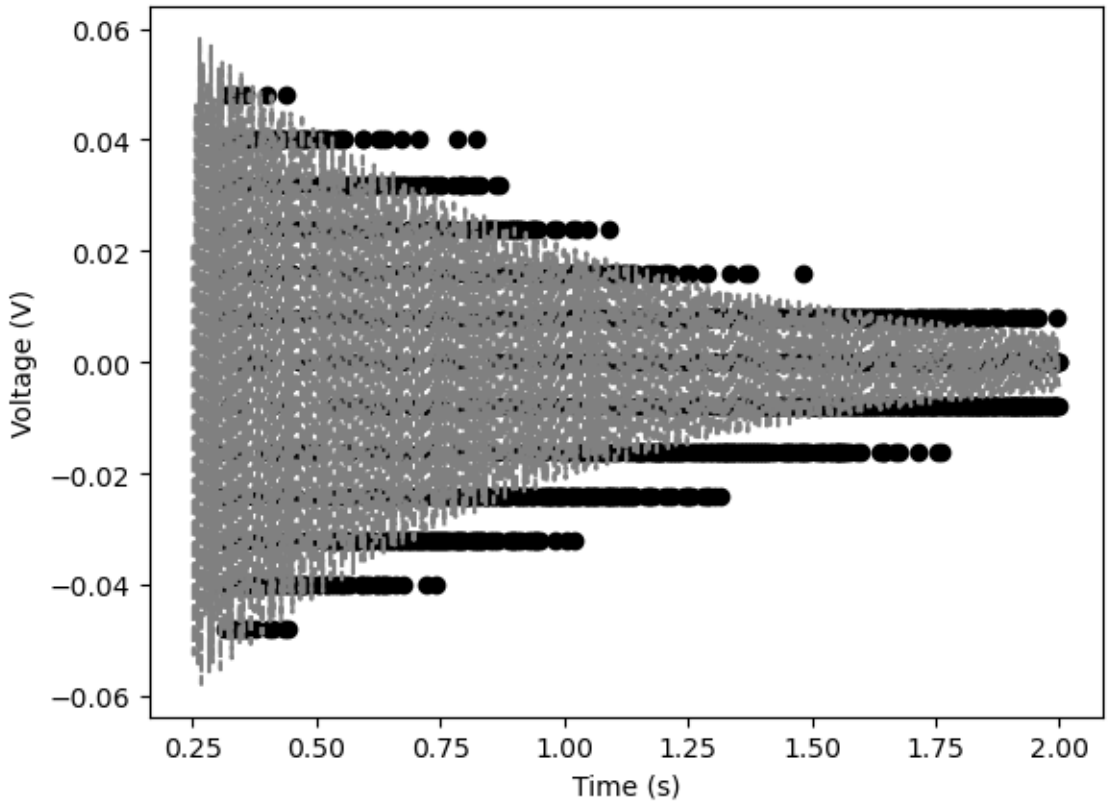

Figure 24: Graph of time (s) vs. voltage (V) with the fit. Notice that it is hard to decipher the individual peaks on the graph of the data. This is due to insufficient data points.

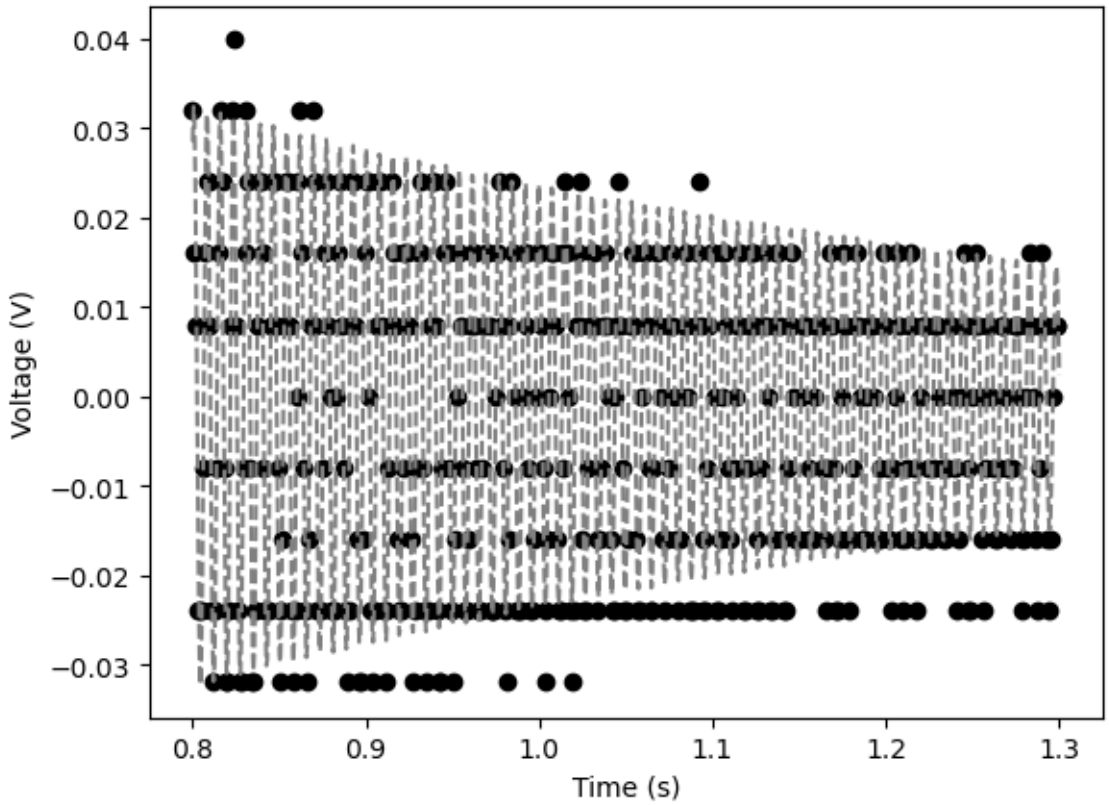

Figure 25: The same fit as in figure 24 but on a smaller section of data.

As can be seen in figure 24 and figure 25, the frequency was not very well resolved, so the procedure was repeated with a signal amplifier in order to determine if the suggested value for the frequency was a good fit. From this signal (figure 26), a frequency was obtained which generally agreed with the frequency initially guessed by the fit (figure 27).

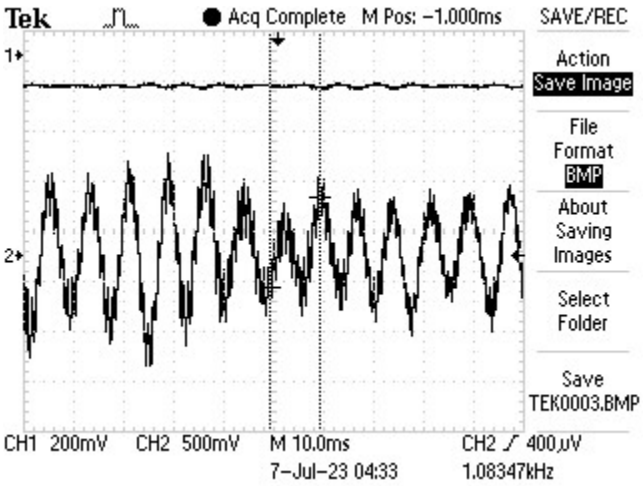

Figure 26: Oscilloscope signal of the laser oscillation after adding a signal amplifier.

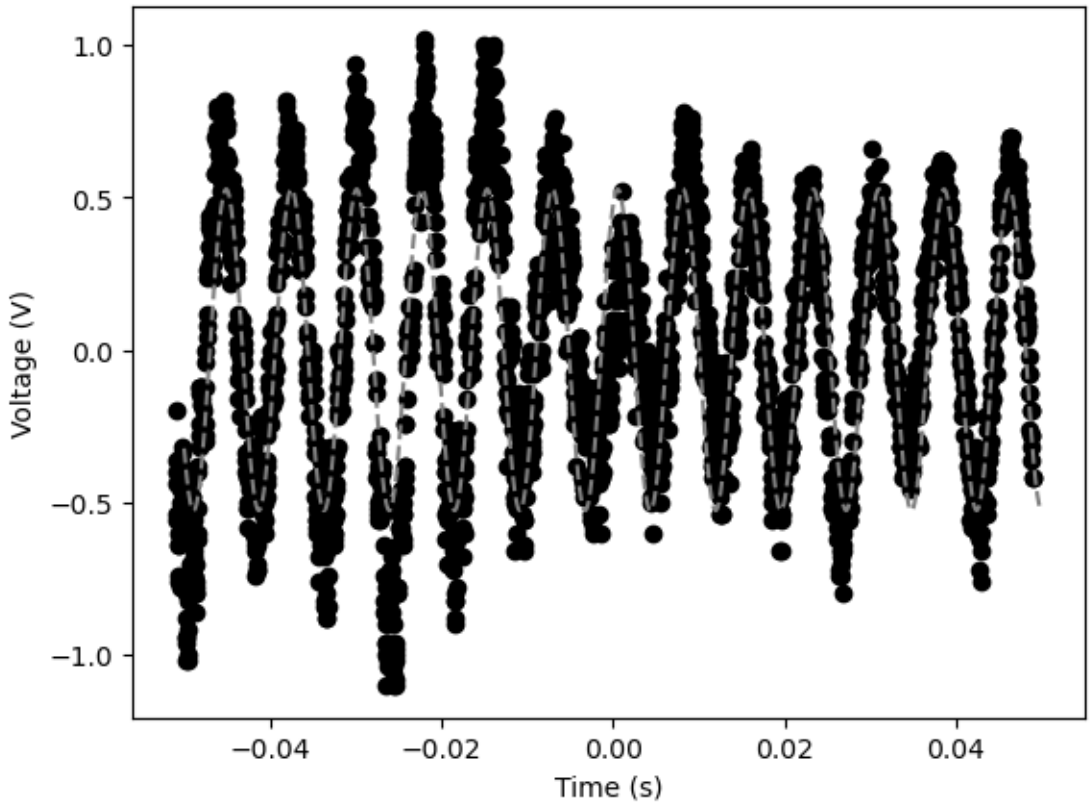

Figure 27: A fit of the laser oscillation after amplifying the signal. Notice the fit clearly lines up well with the frequency of the data points.

A least squares fit was performed to get a sense of how the fit for the data should look. After getting an idea for the range of the parameters, a Bayesian inference with Monte Carlo sampling was performed to obtain a probability distribution.

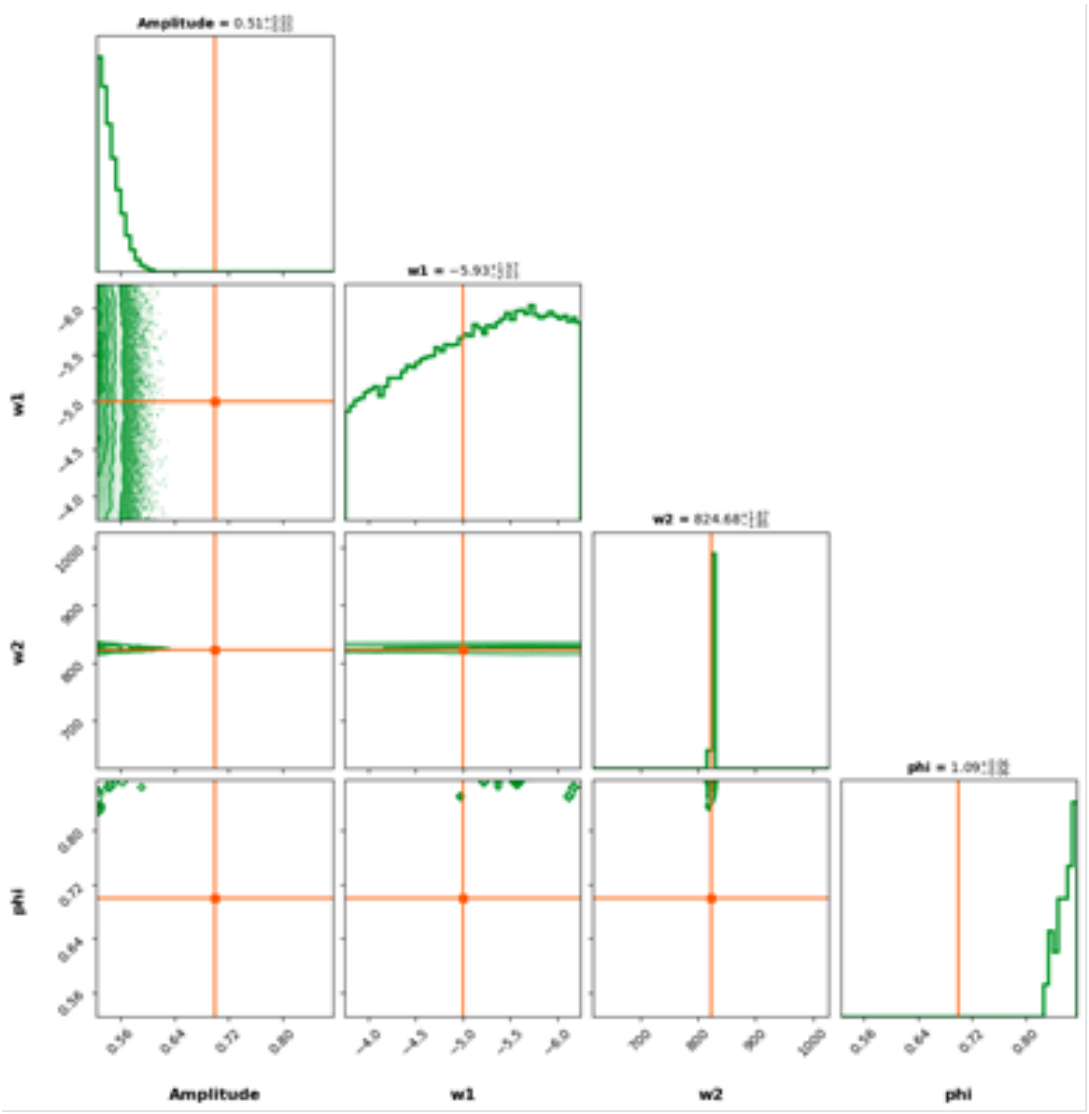

Figure 28: A corner plot showing the posterior distributions for each parameter. Note that the data was fit to the equation $Ae^{w1*t}\sin(w2*t)$.

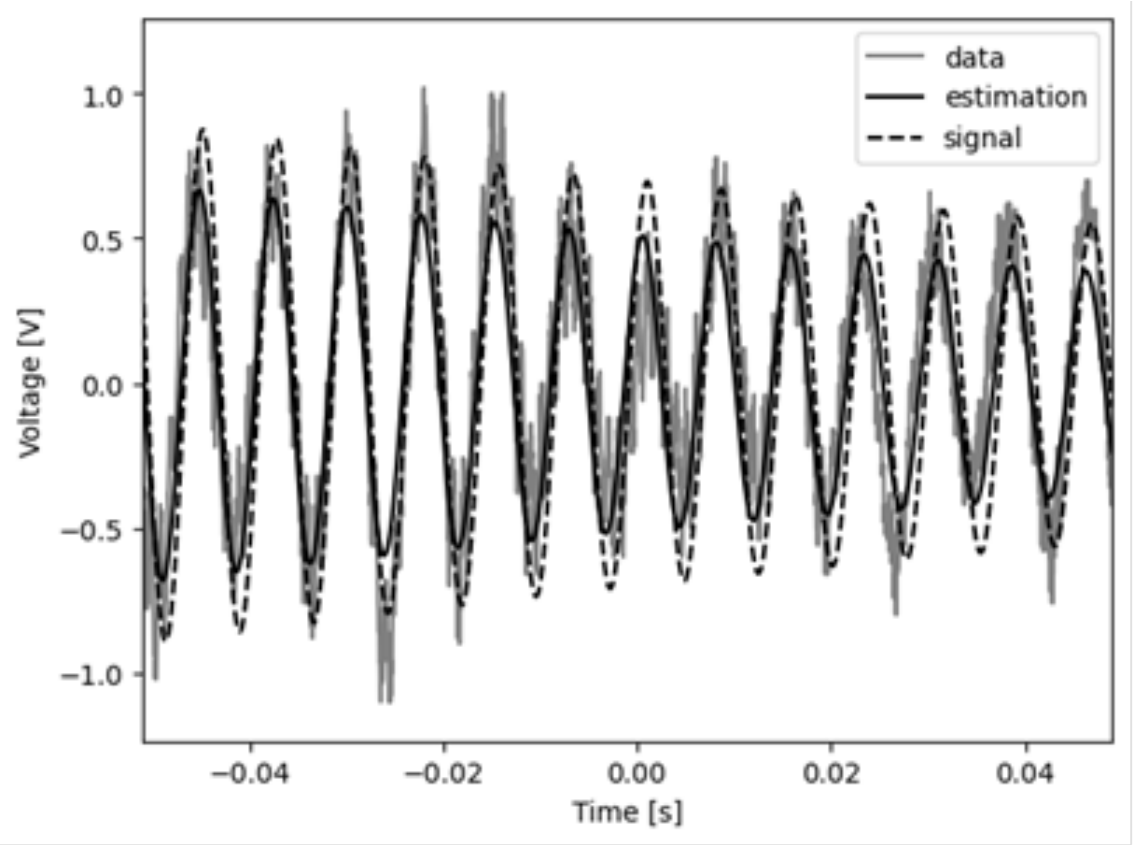

Figure 29: The fit plotted against the data where the signal is the least squares fit and the estimation is from the Bayesian inference.

Calculated Q from initial guessed signal: 82.2
Calculated Q from estimated signal: 69.5

4 Problems

I have additional data which is not included in this report and which was difficult to fit due to there being a background sine wave. I attempted to remove the background wave by fitting a sine wave to it and subtracting it from the data with not much success. After examining the experimental setup, I found that the laser was pulsing, causing there to be a sine wave when the cantilever was not oscillating. After the cantilever is modelled, the experiment will be repeated with a new laser.

5 Goals

When the cantilever is oscillated, some energy is lost through friction with the clamp. Modelling the clamp with the same finite element analysis would help us reduce this loss.

I would also like to improve my fit of the data I gather so the error in our estimates can be reduced.

References

[1] Cesarini, E., Lorenzini, M., Cagnoli, G., Piergiovanni, F. (2009). A gentle nodal suspension for measurements of the acoustic attenuation in materials. *2014 IEEE Metrology for Aerospace (MetroAeroSpace)*, 528-532.

[2] Douglas, R., *Aspects of hydroxide catalysis bonding of sapphire and silicon for use in future gravitational wave detectors*. (2017).

[3] Wright, J. J. Zissa, *D. E. OPTICAL CONTACTING FOR GRAVITY PROBE STAR TRACKER*. 14 (1984).

[4] Zawada, A., *Final Report: In-Vacuum Heat Switch*. 14.